Engineered multiwavelength conversion using nonperiodic optical superlattice optimized by genetic algorithm

Jui-Yu Lai,[1] Yi-Jhen Liu,[1] Yen-Hung Chen,[2] Shang-Da Yang[1,*]
[1]*Institute of Photonics Technologies, National Tsing Hua University, Hsinchu 30013, Taiwan*
[2]*Department of Optics and Photonics, National Central University, Jhongli 320, Taiwan*
**Corresponding author: shangda@ee.nthu.edu.tw*

Abstract: Nonperiodic optical superlattice for multiwavelength conversion with flexible spectral distributions is optimized by genetic algorithm using two target functions sequentially. The overall conversion efficiency could be higher than that of aperiodic optical superlattice by 14%.

OCIS codes: (190.4360) Nonlinear optics, devices, (230.7405) Wavelength conversion devices

1. Introduction:

Quasi-phase-matching (QPM) in ferroelectric materials has been widely used in a variety of wavelength conversion processes [1]. In some applications, such as gas sensing using several absorption lines [2] and equalized wavelength conversion grids [3], multiple phase-matching (PM) spectral peaks with unequal spacing and different heights are required, which cannot be accomplished by some of the existing methods [3,4,5]. Aperiodic optical superlattice (AOS) optimized by simulated annealing (SA) [6] can meet the aforementioned requirements, but the domain size is limited to integral multiples of some unit block length. In contrast, nonperiodic optical superlattice (NOS) [7] removes the domain size restriction, and is expected to achieve better conversion efficiency and design fidelity. However, the NOS in [7] can only produce PM peaks of equal height and has to be optimized by the combination of SA and genetic algorithm (GA). Here we demonstrate NOS solely optimized by GA to achieve PM peaks of unequal spacing and different heights. Our simulations show a 14% efficiency improvement compared to that obtained by AOS of the same length. We have also investigated the distortion of PM tuning curve in the presence of fabrication errors and pump depletion, and are making QPM lithium niobate crystals for experimental demonstration.

2. Theory:

Without loss of generality, we demonstrate the NOS scheme by examining second-harmonic generation (SHG) in a lithium niobate bulk of length L. The crystal is divided into N blocks with different lengths (to be optimized), and adjacent blocks have opposite domain orientations. If the pump is non-depleted, the conversion efficiency spectrum is given by [7]:

$$\eta(\lambda) = \eta_{norm}(\lambda) \cdot d_{eff}^2(\lambda), \quad d_{eff}(\lambda) = \frac{1}{L}\left|\int_0^L \tilde{d}(x) e^{i\Delta k(\lambda)\cdot x} dx\right|, \tag{1}$$

where λ is the fundamental wavelength, η_{norm} is the normalized efficiency in units of %/W, d_{eff} is the effective nonlinear coefficient determined by the NOS design, Δk is the wave vector mismatch, and $\tilde{d}(x)$ (taking values of 1 or -1) represents the spatial distribution of domain orientation. To achieve multiple PM peaks at specified wavelengths $\{\lambda_\alpha\}$, we sequentially employ two target functions T_1, T_2 in search of an optimized $\tilde{d}(x)$ by GA:

$$T_1 = \sqrt{\sum_\alpha \left[\eta_\alpha - \eta_\alpha^{(0)}\right]^2}, \qquad T_2 = T_1 + \sum_\alpha \left|\eta_\alpha - \eta_{tot} \cdot \eta_\alpha^{(0)}\right|, \tag{2}$$

where $\eta_\alpha^{(0)}$ ($\sum \eta_\alpha^{(0)} = 1$) and η_α represent the desired and achieved conversion efficiencies at λ_α normalized to the peak efficiency η_{unif} due to a uniform QPM grating of the same length L, and $\eta_{tot} = \sum \eta_\alpha$ (<1) denotes the achieved overall efficiency. Our simulations show that minimizing T_1 can only suppress conversion efficiencies at undesired wavelengths ($\lambda \notin \{\lambda_\alpha\}$), while the resulting PM spectral shape is typically unsatisfactory. This problem can be solved by preserving the elite individuals identified by T_1 and subsequently using T_2, where the factor η_{tot} is used to dynamically damp the desired conversion efficiencies $\eta_\alpha^{(0)}$ without distorting the relative distribution. In this way, the evolution power of GA can be dedicated to improving the PM spectral shape. In our algorithm, a fixed number of generations N_i is specified for target function T_i, (i=1, 2) in advance.

3. Simulation and discussion:

In all of our NOS designs, we used 200 individuals for each of the 8 subpopulations, 2000 blocks per individual, and required that no domain size is less than 4.5 μm (in view of the typical limitations of high-quality e-field poling). Fig. 1 (solid) shows the V-shaped PM tuning curve $\eta(\lambda)/\eta_{unif}$ (consisting of five equally-spaced peaks) of an NOS optimized by GA with the simulation parameters $\{\eta^{(0)}\}$={0.267, 0.183, 0.1, 0.183, 0.267}, N_1=6000, N_2=500. The overall efficiency η_{tot} is 0.87, meaning that 87% second-harmonic power lies in the specified wavelengths. The five peak efficiencies η_α only slightly differ from the corresponding ideal values $\eta_{tot}\cdot\eta_\alpha^{(0)}$ (circles) with a small average error $\Delta\eta$ ($\equiv \sum_\alpha \left|\eta_\alpha - \eta_{tot}\cdot\eta_\alpha^{(0)}\right| / \eta_{tot}$)=1.54%, showing good fidelity in PM spectral shape. Without using the second target function T_2, however, we arrived at a result (not shown here) with lower efficiency (η_{tot}=0.74) and much worse fidelity ($\Delta\eta$=10.6%). The histogram of domain length of the NOS (inset) has a bell-shaped distribution centered around 9.5 μm, consistent with the ~19-μm QPM period for SHG of ~1550 nm in a lithium niobate bulk. We also designed an AOS of the same length (L=1.89 cm) with unit block size of 4.82 μm for comparison. The resulting PM tuning curve (dash) has an overall efficiency η_{tot}=0.75 (lower than that of the NOS by 14%) and a similar fidelity $\Delta\eta$=1.14%. The corresponding histogram of domain length (not shown here) indicates that most (93%) of the AOS domains consist of two unit blocks (9.64-μm-long), while the specific PM spectral shape is achieved by the allocation of a small fraction (7%) of the domains, limiting the performance of AOS design.

To show the flexibility of NOS, we designed another device to achieve three unequally-spaced PM spectral peaks with identical height. The simulation parameters are $\{\eta^{(0)}\}$={0.33, 0.33, 0.33}, N_1=5000, N_2=400. The resulting PM tuning curve (Fig. 2, solid) corresponds to an overall efficiency η_{tot}=0.76 (similar to that in Reference [6]), and a nearly perfect fidelity (variation of the three peak efficiencies is ~10^{-7}). We also investigated the performance of NOS in the presence of fabrication errors, such as the uniform domain broadening (shrinking) due to overpole (underpole) in the poling process, and the random variation in domain size due to uncontrollable factor in each block. With a domain broadening error Δx=+0.7 μm and a normally distributed domain size error of standard deviation δx =0.7 μm [6], the resulting PM tuning curve (Fig. 2, dash) corresponds to an overall efficiency of η_{tot}=0.71 (lower than that of the error-free device by 5.7%) and a slightly deteriorated fidelity of $\Delta\eta$=0.28%. This result is in agreement with those in Reference [6] and our simulations about V-shaped PM tuning curve produced by NOS and AOS, showing that our scheme is highly insensitive to typical fabrication errors.

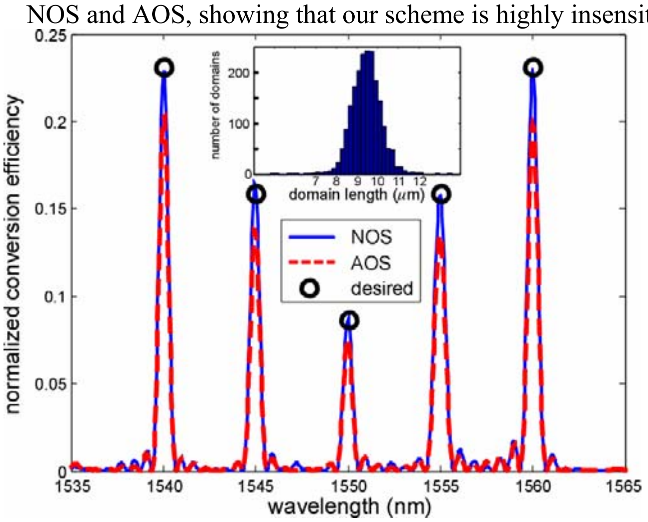

Fig.1. V-shaped normalized PM tuning curve of NOS (solid) and AOS (dash). The inset shows the histogram of domain length of the NOS.

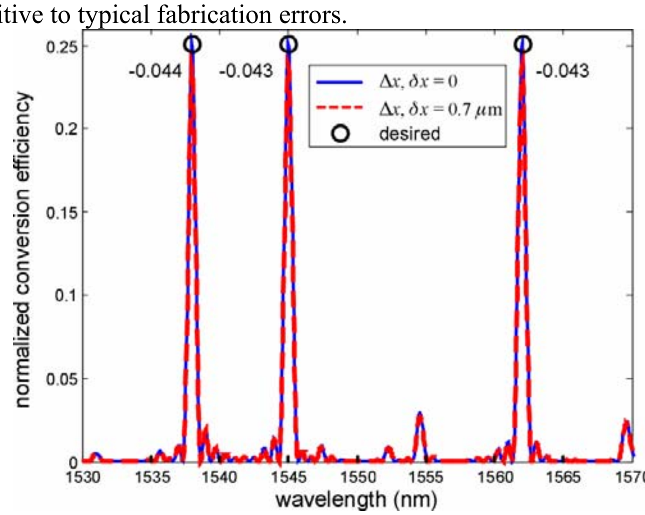

Fig.2 Normalized PM tuning curve without (solid) and with (dash) fabrication errors. The values near the peaks represent the reduction of normalized efficiency between these two cases.

The authors gratefully thank constructive comments from Y.-C. Huang and R.-K. Lee. This work is supported by the National Science Council of Taiwan under grant 97-2221-E-007-028 and 97-2221-E-008-030.

References

1. D. S. Hum, M. M. Fejer, C. R. Physque **8**, 180 (2007).
2. M. Asobe, et. al., Opt. Lett., **32**, 3388 (2007).
3. C. R. Fernandez-Pousa, et. al., IEEE PTL, **17**, 1037 (2005).
4. M. H. Chou, et. al., Opt. Lett., **24**, 1157 (1999).
5. M. Asobe, et. al., IEEE J. Quantum Electron., **41**, 1540 (2005).
6. Y. W. Lee, et. al., Opt. Lett., **27**, 2191 (2002).
7. X. Chen, et. al., Phys. Rev A., **69**, 013818, (2004).